

## Electronic Supplementary Information (ESI)

### Fluoride free synthesis of anatase TiO<sub>2</sub> nanocrystals with exposed active {001} facets

Narottam Sutradhar, Abul Kalam Biswas, Sandip K. Pahari, Bishwajit Ganguly\*, Asit Baran Panda\*

#### Detailed Synthetic procedure.

##### Materials.

Titanium iso-propoxide was purchased from Sigma Aldrich, USA. Ethanol, ammonium carbonate, 30% hydrogen peroxide, p- nitrotoluene, methylene blue was purchased from S. D. Fine-Chem. Limited, India. All the chemicals were used without further purification. For all applications water with a resistivity of 18 MΩ cm was used, obtained from a Millipore water purifier.

##### Preparation of TiO<sub>2</sub> nanoparticles.

The titanium hydroxide was precipitated from 0.01 mole titanium iso-propoxide. At first iso-propoxide was mixed in 17ml of methanol to which Millipore water was added slowly with constant stirring at 300 rpm. A white precipitate appeared immediately after the addition of water and stirring was continued for another 15min. The resultant precipitate was collected by filtration and washed for 4 times using de-ionized water. Then, 25 ml 1.6 molar aqueous ammonium carbonate solutions was added to the resultant precipitate with constant stirring. To this milky white reaction mixture, 3 ml 30% H<sub>2</sub>O<sub>2</sub> was added which resulted a light yellow coloured clear precursor solution with a pH of ~9.2. To this solution dilute aqueous NaOH solution was added drop wise until pH reached to 10. The final volume of the solution was made to 40ml. The solution was then subjected to hydrothermal treatment (HTT) in teflon lined steel autoclave at 200°C for 6 hrs. The resultant precipitate was collected by centrifuge, washed several times with de-ionized water and dried at ambient conditions overnight.

### Controlled Reactions:

In order to establish the terminating effect of 001 facet by  $\text{CO}_3^{2-}$  ion, layered titanate synthesized at room temperature was treated hydrothermally in presence of individual adsorbents, i.e.,  $\text{H}_2\text{O}$ ,  $\text{NH}_4\text{OH}$  and  $\text{CO}_2$ . For this Protonated layered titanate (PLT) was prepared as reported in our previous work,<sup>1-2</sup> washed and dried at ambient condition. In two separate experiment 300 mg of PLT was dispersed in 40 water and  $\text{NH}_4\text{OH}$  and treated hydrothermally at  $200^\circ\text{C}$  for 24 hours. In an experiment 300 mg PLT was dispersed in  $\text{H}_2\text{O}$  and subjected to HTT under  $\text{CO}_2$  atmosphere of 10 bars for 24 hours at  $200^\circ\text{C}$ . The entire products resulted phase pure anatase  $\text{TiO}_2$ . TEM images confirmed the formation of single crystalline individual nanoparticles, with a particle size range of 30-50 nm. However nanoparticle synthesized in presence of  $\text{CO}_2$  showed the decahedron anatase  $\text{TiO}_2$ , with dominant  $\{001\}$  facets, whereas that in presence of  $\text{NH}_4\text{OH}$  and  $\text{H}_2\text{O}$  yielded octahedron shaped anatase particles with dominant 101 facets.

### Photocatalytic reaction Procedure:

Photocatalytic degradation of organic compounds was carried out using a reactor that consists of a double-wall quartz jacket with an inlet and an outlet for water circulation to maintain the temperature of the reaction mixture. It also has an empty chamber at the centre where a 125 W high-pressure mercury vapour lamp is kept as the UV source. The spectral response of the subject UV source is as shown in Figure 1. The second part is the outer borosilicate glass container (volume 250 ml after insertion of the inner part) in which the reaction takes place. The whole set up is placed on a magnetic stirrer inside a wooden chamber under continuous stirring to maintain uniform dispersion of the solid catalyst.

Photocatalytic reaction was carried out with a catalyst concentration of 0.2 g/L, and a starting concentration ( $C_0$ ) of  $7.3 \times 10^{-4}$  mol/L of the pollutant para-nitrotoluene (PNT). Prior to irradiation, the dispersions in the glass vessels were magnetically stirred in the dark for ca. 30 min for the establishment of an adsorption/desorption equilibrium. At regular irradiation time intervals, samples (4 ml) were withdrawn by syringe from the irradiated suspension up to 4 hrs, centrifuged at 15000 rpm to separate the  $\text{TiO}_2$  particles. Concentration of remaining organic compound in the solution was determined by a UV-visible spectrophotometer (Shimadzu-160A).

### Characterization.

X-ray diffraction analysis was carried out with a Philips X'pert MPD System in the  $2\theta$  range of the  $10-60^\circ$  at a scan speed of  $3^\circ \text{ min}^{-1}$  using  $\text{Cu K}\alpha$  ( $\lambda = 1.54056 \text{ \AA}$ ) was used. The diffraction patterns obtained was compared with that of the JCPDS data of standard anatase, rutile brookite and layered titanate diffractogram. Careful analysis of the products obtained at different conditions confirmed the formation mainly two distinct phase of titanium oxide namely layered dititanate and anatase. Crystallite size of the anatase particles (Table-1) were measured using Scherer formula, with a shape factor (K) of 0.9

$$\text{Crystallite size} = K\lambda / W \cos \theta$$

Here  $W = W_b - W_s$ ,  $W_b$  is the broadened profile width if the experimental,  $W_s$  is the standard profile width of the reference silicon sample, and  $\lambda$  is the wave length of X-ray radiation Cu K $\alpha$  ( $\lambda = 0.154056$  nm).

The nitrogen adsorption - desorption measurements at 77 K were performed by using an ASAP 2010 Micromeritics, USA, after degassing samples under vacuum ( $10^{-2}$  torr) at 250 °C for 4 h. The surface area was determined by Brunauer-Emmett-Teller (BET) equation. Pore size distributions were determined using BJH model of cylindrical pore approximation.

A scanning electron microscope (SEM) (Leo series 1430 VP) equipped with INCA was used to determine the morphology of samples. The sample powder was supported on aluminium stubs and then coated with gold by plasma prior to measurement.

Transmission electronic microscope (TEM) images were collected using a JEOL JEM 2100 microscope and samples were prepared by mounting an ethanol dispersed samples on lacey carbon formvar coated Cu grid.

### Computational Methodologies.

All DFT calculations were performed with the program package DMol<sup>3</sup> in Materials Studio (version 4.1) from Accelrys Inc.<sup>3-4</sup> We have used DND (double numerical with  $d$  polarization) and DNP (double numerical with  $d$  and  $p$  polarization) basis sets which are comparable to 6-31G\* and 6-31G\*\* Gaussian-type basis sets, respectively. The optimization of additive on the  $4 \times 4$  slab models of TiO<sub>2</sub> was performed with LDA/PWC/DND level of theory. The single point calculations were reported with GGA/PBE/DNP level of theory.<sup>5-7</sup> The implicit conductor like screening model (COSMO) was employed using the dielectric constant of water (dielectric constant = 78.54) to take into account the solvent effect in these calculations.<sup>8-9</sup> In the case of slabs, the vacuum space is 20 Å. The molecules are adsorbed only one side of the slab. The  $k$  point is only set as  $1 \times 1 \times 1$  as the slabs are large.<sup>10</sup>

**Table S1.** Calculated Adsorption Energy ( $E_{\text{ads}}$ ) (kcal/mol) of the carbonate, ammonia and water over (001) and (101) surfaces.

Surface condition	Monodentate coordination of carbonate to a single Ti <sup>+4</sup> ion	Bidentate coordination of carbonate to two Ti <sup>+4</sup> ions	NH <sub>3</sub> on TiO <sub>2</sub>	H <sub>2</sub> O on TiO <sub>2</sub>
101	−79.12	−96.05	−14.87	−2.33
101	−69.36	−70.27	−20.04	−11.67

**Table S2.** Displacements of the atoms in the uppermost layer, normal to the surface are given in Å.

Surface	Label	Coordination	Ref 5	This work	Fluorated	Carbonated
{001}	O1	2	0.08	0.07	-0.46	-0.68
	O2	3	-0.06	-0.02	0.08	0.01
	Ti1	5	-0.02	-0.07	0.23	0.08
{101}	O1	2	-0.02	-0.02	-0.07	0.02
	O2	3	0.19	0.15	-0.04	-0.55
	Ti1	5	-0.18	-0.16	0.21	0.14

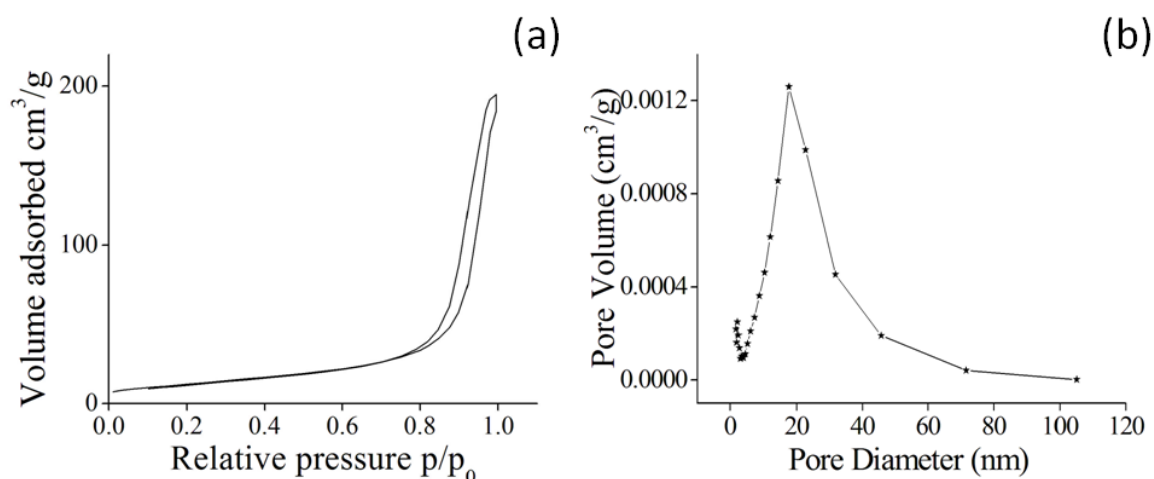


**Fig. S1** N<sub>2</sub> sorption-isotherm (a) and pore size distribution (b) of 001 exposed anatase TiO<sub>2</sub> nanocrystals.

[Fig. S1](#) represents the nitrogen adsorption-desorption isotherms of the synthesized TiO<sub>2</sub> nanoparticles. The isotherm is similar to type II and the hysteresis loop is almost H3 type, (according to the IUPAC classification), generally observed for interparticle pores. The product has a surface area of 47.2 m<sup>2</sup>g<sup>-1</sup>.

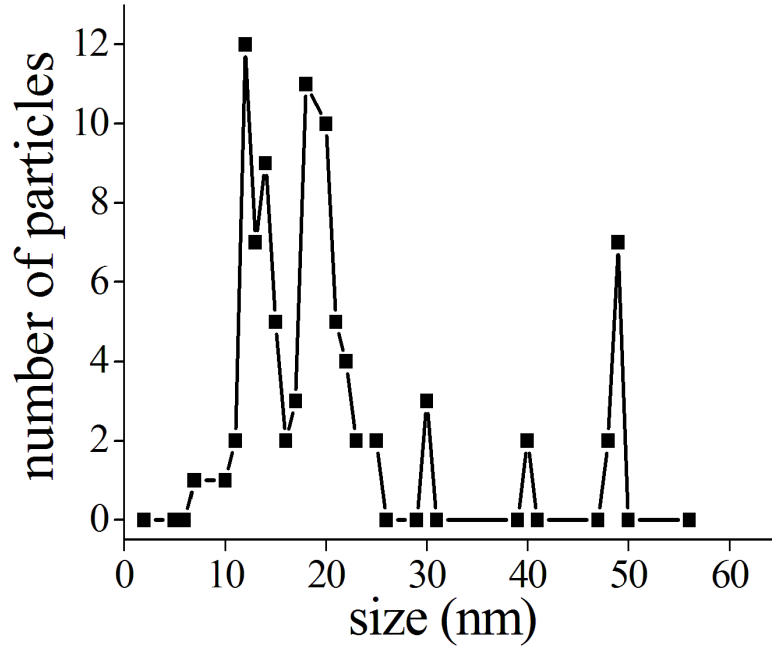


**Fig. S2** Size distribution of the anatase single crystals determined by measurement of 100 anatase particle.

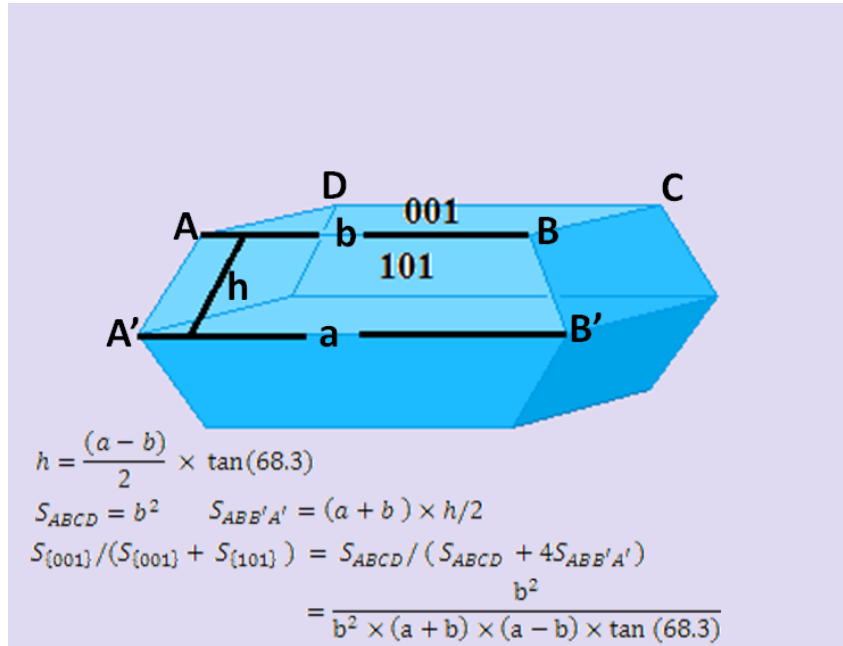


**Fig. S3** Model of anatase TiO<sub>2</sub> decahedral nanocrystals used for calculating the percentage of exposed {001} facets.

The percentage of exposed {001} facets was calculated from the equation of  $S_{\{001\}} / (S_{\{001\}} + S_{\{101\}})$   $= b^2 / [b^2 + (a + b) \times (a - b) \times \tan(68.3^\circ)]$  where  $a$  and  $b$  are the average sizes measured from ~100 (hundred) hexagonal particles<sup>11</sup> which are found to be an average of 21 nm and 16 nm, respectively and was estimated as ~35%.

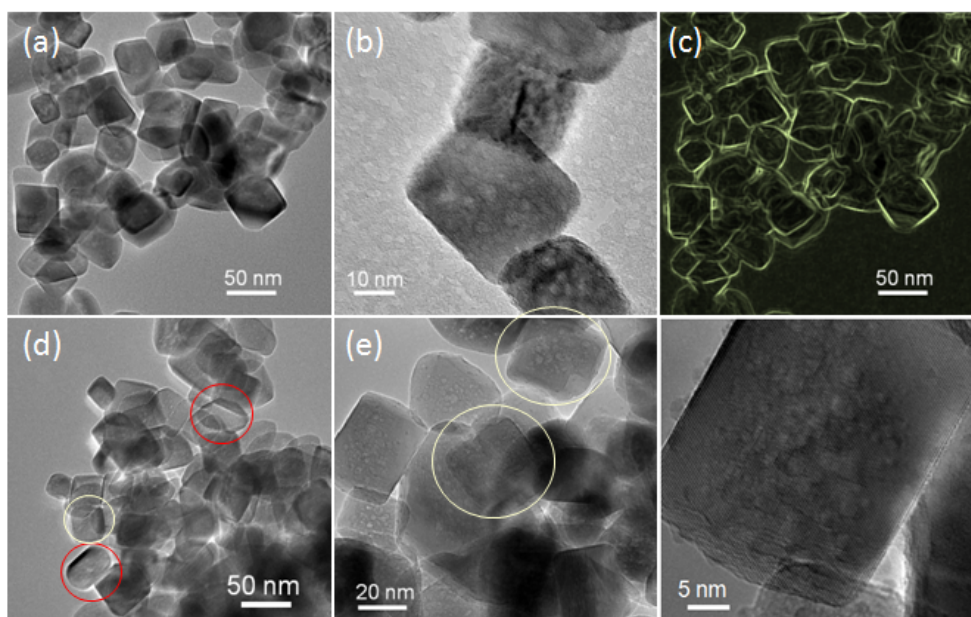


**Fig. S4** TEM images of the anatase  $\text{TiO}_2$  single crystals prepared at  $250^\circ\text{C}$ .

TEM indicate the enhancement of particle size ( $> 40$  nm) with a higher degree of truncation on increase in processing temperature. In the TEM images presence of distinct shapes, (square, hexagon and rhombus) due to highly truncated octahedral (bi-pyramidal) particles (decahedral structure) viewing in different direction, i.e., zone axis ( $[001]$ ,  $[010]$  and  $[111]$ ) are marked my circle.

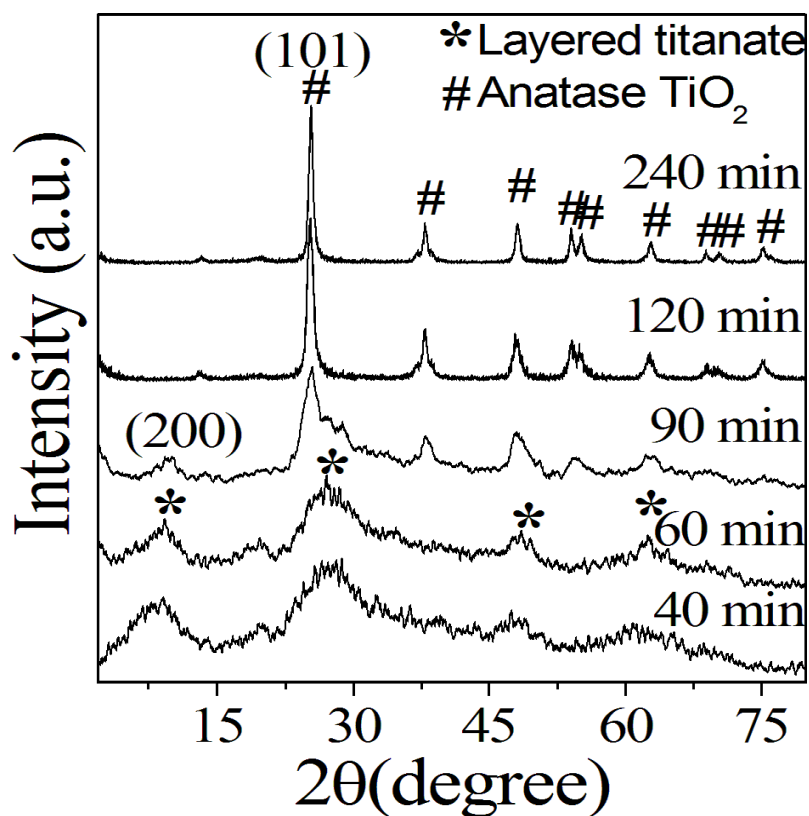


**Fig. S5** XRD pattern of intermediates during hydrothermal treatment of precursor solution at  $200^\circ\text{C}$ .



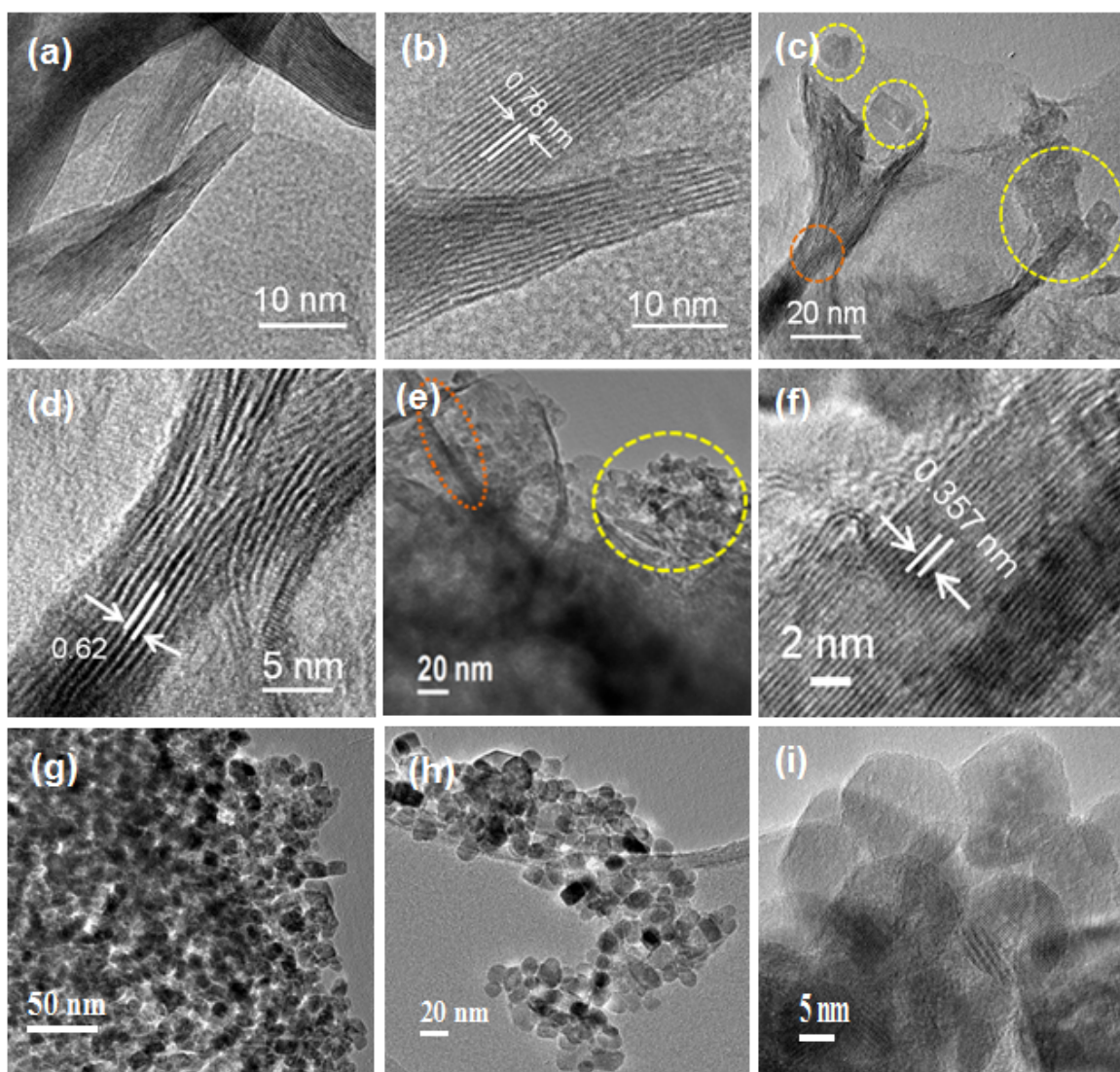


**Fig. S6** Time resolved TEM and HR-TEM images of the products obtained via hydrothermal treatment of PTC precursor at 200°C after 60 minutes (a, b), 90 minutes (c, d), 120 minutes (e, f, g), 240 minutes (h, i), and 240 minutes (h, i).

From the time resolved TEM images, it is evident that only 2D layered structure was observed in 60 min. The layers are nothing but a stack of sheets, which was confirmed in the edge-curved position of the sheets (Figure S5a). The interlayered distances are 0.78nm, which is almost equivalent to the as synthesized layered titanate (Figure S5b). In 90min, very little amount of small particles (yellow circle) were observed with sheet (orange circle) (Figure S5c). During this time (60-90 min) i.e. phase transformation (as per XRD), layered structure was collapsed partially and inter layered spacing was decreased to 0.62nm (Figure S5c). After 120 min, mainly aggregated nanoparticles (10-15nm, yellow circle) were identified (Figure S5e, g) with little amount of sheet morphology (orange circle, (Figure S5e, f). Inter layered spacing was further decreased to 0.357nm, which is equal to the lattice spacing of (101) plane of anatase  $\text{TiO}_2$ . As a result, respective peak of layered structured was identified in XRD pattern. After 4 h b (240min), the layered structure was fully collapsed and intermediate of only well faceted decahedral nanoparticles (obtained after 24h) were identified (Figure S5h, i).

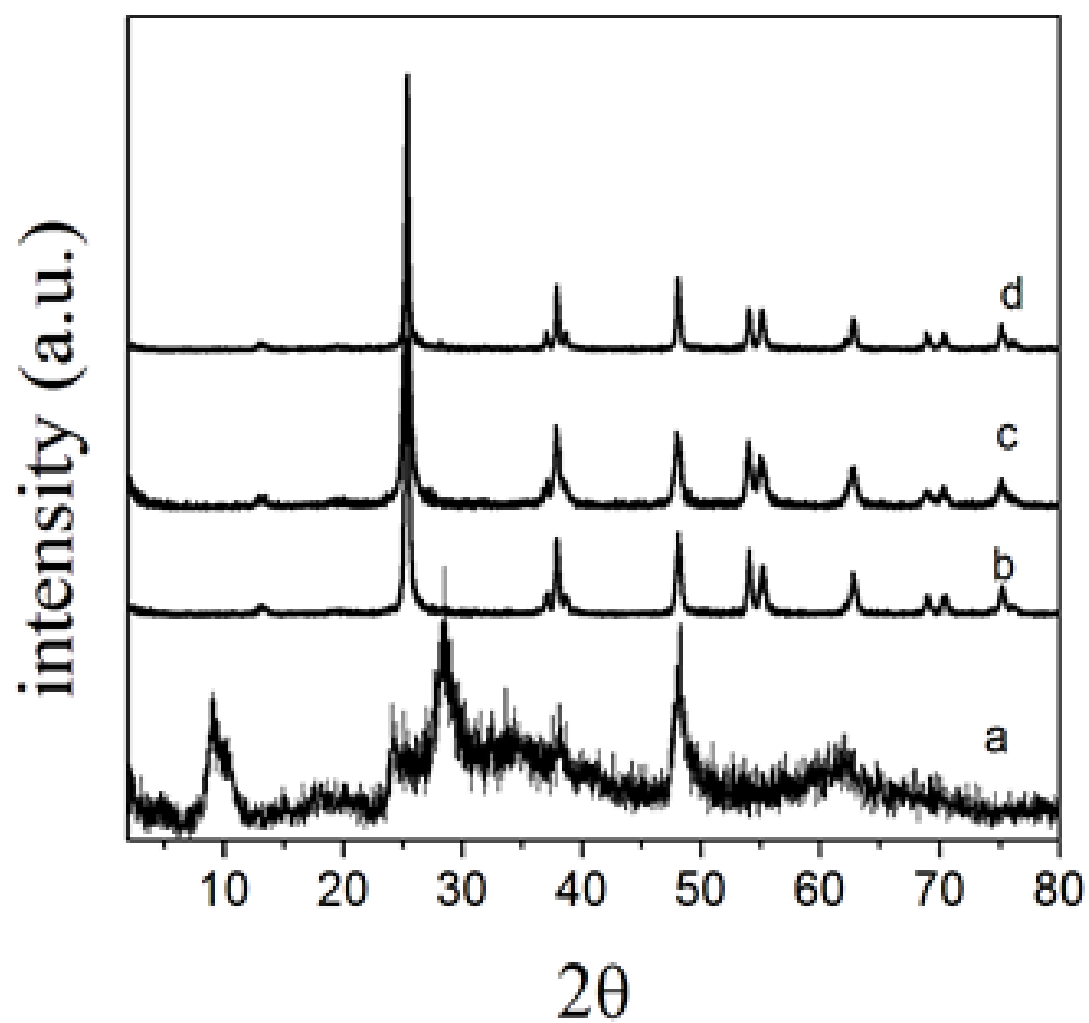


**Fig. S7** X-ray diffraction pattern of (a)  $\text{TiO}_2\text{-NaOH}$ , (b,)  $\text{TiO}_2\text{-NH}_3$ , (c) $\text{TiO}_2\text{-CO}_2$ , (d)  $\text{TiO}_2\text{-H}_2\text{O}$ .



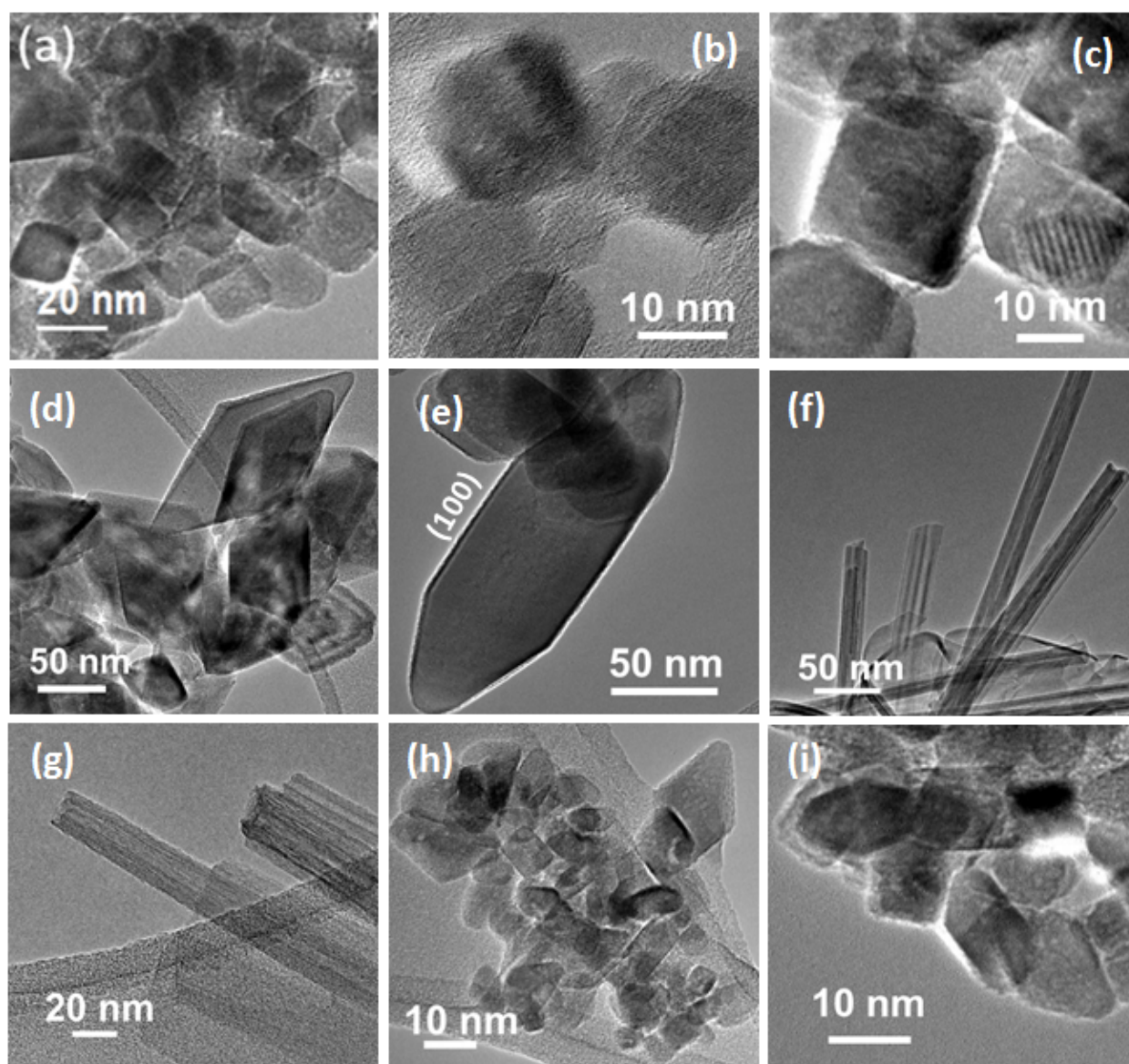


**Fig. S8** TEM images of the samples synthesized through the hydrothermal treatment of layered titanate (synthesized at room temperature) in the presence of  $\text{H}_2\text{CO}_3$  ( $\text{CO}_2+\text{H}_2\text{O}$ ) (a, b, c),  $\text{NH}_4\text{OH}$  (30 %,  $\text{NH}_3+\text{H}_2\text{O}$ ) (d, e),  $\text{NaOH}$  (f, g) and  $\text{H}_2\text{O}$  (h, i).

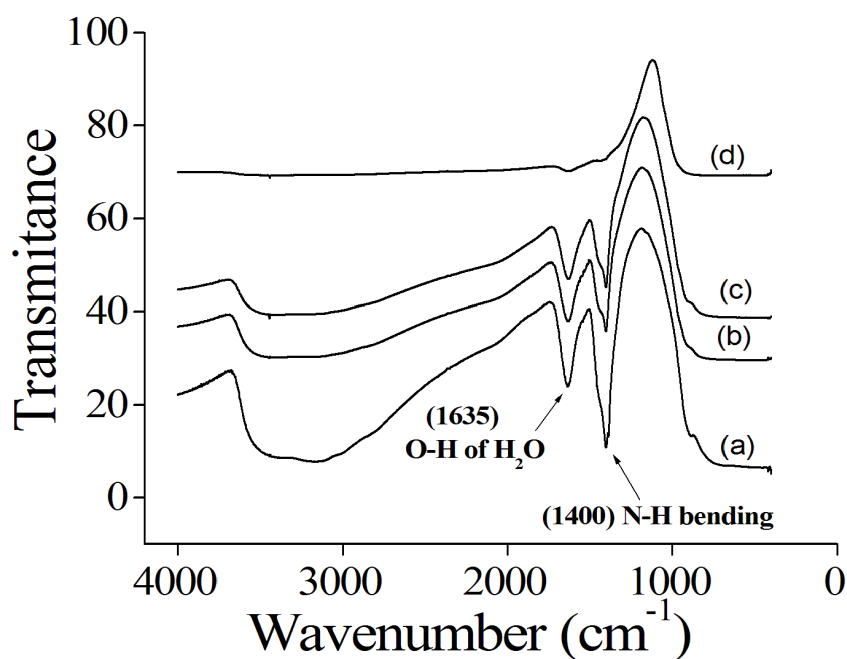


**Fig. S9** IR absorption spectra of (a) TiO-200/40min, (b) TiO-200/60min, (a) TiO-200/90min and (a) TiO-200/120min.

With increasing in the hydrothermal treatment time the ammonium ions were escaped as ammonia from the solution, as in an aqueous ammonia thermodynamic system, temperature and time governs the balance between free ammonia and ammonium ions. Due to insufficient ammonium ions, the system cannot provide sufficient positive charge to stabilize negatively charged titanate layers and the interlayer spacing was decreased gradually. The displacement of ammonium ion was further supported by the FT-IR spectroscopic study of intermediates. In the IR spectrum of intermediates with varying time, the intensity of the bands at 3620–3630  $\text{cm}^{-1}$  region for vibrations of hydroxyl groups, bound at 1400  $\text{cm}^{-1}$  for N–H bending and at 2800 to 3400  $\text{cm}^{-1}$  for N–H stretching, can be attributed to the  $\text{NH}_4^+$  ions, were gradually decreased and finally disappeared at 2h .

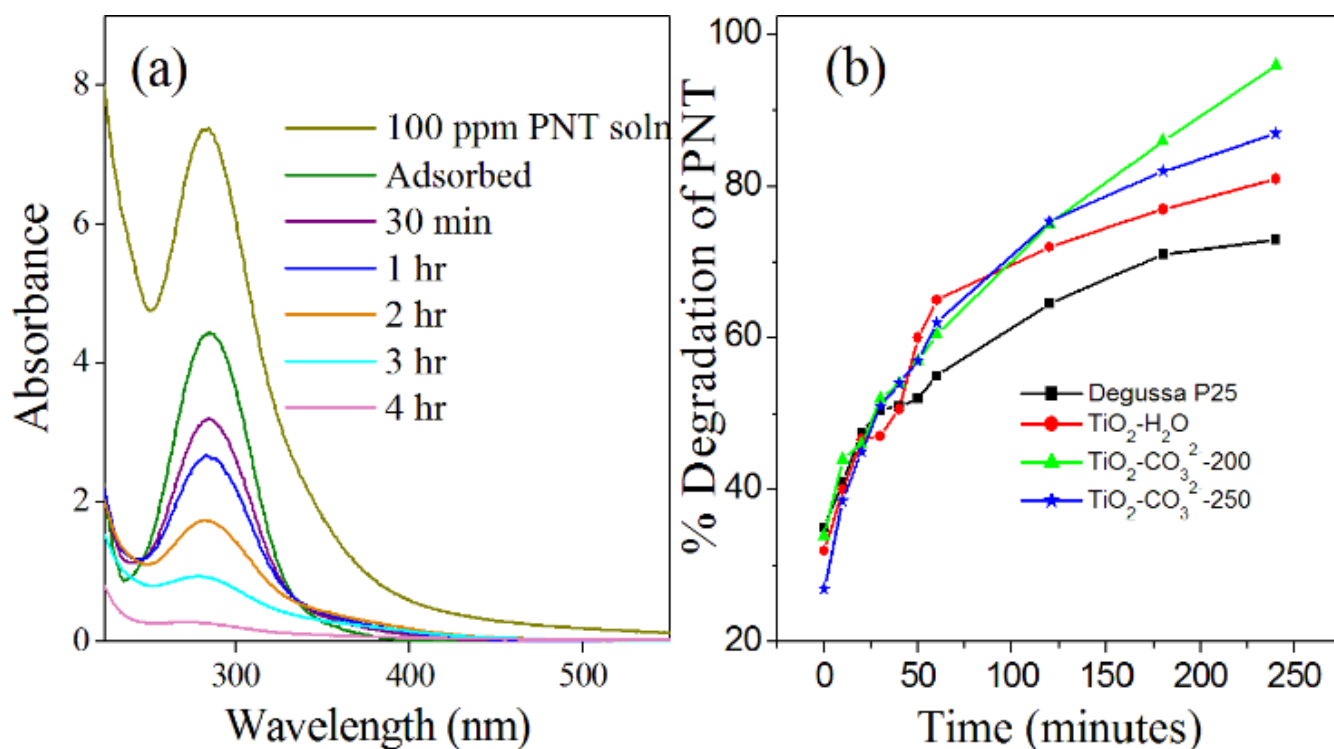


**Fig. S10.** (a) UV adsorption curve of the solutions of p-nitritoluene degraded for various time intervals using anatase  $\text{TiO}_2\text{-CO}_3\text{-200}$ . (b) Rate of degradation of 250 ml 100 ppm p-nitritoluene with Degussa P-25,  $\text{TiO}_2\text{-H}_2\text{O}$ ,  $\text{TiO}_2\text{-CO}_3\text{-200}$  and  $\text{TiO}_2\text{-CO}_3\text{-250}$ .

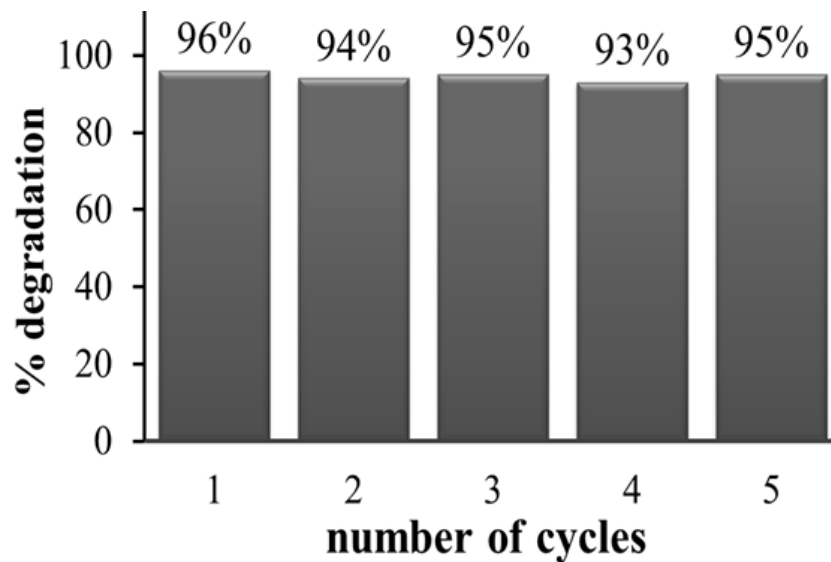


**Fig. S11** Bar plot of percentage degradation of 250 ml 100 ppm p-nitritoluene upto 5 th cycle showing reusability of the synthesized  $\text{TiO}_2$ .

## References:

1. N. Sutradhar, A. Sinhamahapatra, S. K. Pahari, H. C. Bajaj and A. B. Panda, *Chem. Commun.* 2012, **147**, 7731.
2. N. Sutradhar, S. K. Pahari, M. Jayachandran, A. M. Stephan, J. R. Nair, B. Subramanian, H. C. Bajaj, H. M. Mody and A. B. Panda, *J. Mater. Chem. A* 2013, **1**, 9122.
3. *Materials Studio* DMOL3 Version 4.1, Accelrys Inc., San Diego, CA.
4. B. Delley, *J. Chem. Phys.* 2000, **113**, 7756.
5. Z. Wu, R. E. Cohen and D. Singh, *J. Phys. Rev. B* 2004, **70**, 104112.
6. P. Ziesche, S. Kurth and J. P. Perdew, *Comput. Mater. Sci.* 1998, **11**, 122.
7. W. Kohn, A. D. Becke and R. G. Parr, *J. Phys. Chem.* 1996, **100**, 12974.
8. A. Klamt, COSMO and COSMO-RS. In *Encyclopedia of Computational Chemistry*; von Rague Schleyer, P., Allinger, N. L., Eds.; Wiley: New York. **2**, 604 (1998).
9. A. Klamt, *J. Phys. Chem.* 1995, **99**, 2224.
10. H. G. Yang, G. Liu, S. Z. Qiao, C. H. Sun, Y. G. Jin, S. C. Smith, J. Zou, H. M. Cheng and G. Q. Lu, *J. Am. Chem. Soc.* 2009, **131**, 4078–4083.
11. J. S. Chen, Y. L. Tan, C. M. Li, Y. L. Cheah and D. Luan, *J. Am. Chem. Soc.*, 2010, **132**, 6124.